Neuron, Vol. 46, 595–607, May 19, 2005, Copyright ©2005 by Elsevier Inc. DOI 10.1016/j.neuron.2005.03.029

# Nicotine Upregulates Its Own Receptors through Enhanced Intracellular Maturation

**Jérôme Sallette, Stéphanie Pons, Anne Devillers-Thiery, Martine Soudant, Lia Prado de Carvalho, Jean-Pierre Changeux,* and Pierre Jean Corringer***
CNRS URA D2182 Récepteurs et Cognition
Institut Pasteur
25 rue du Dr. Roux
75724 Paris Cedex 15
France

## Summary

**Chronic exposure to nicotine elicits upregulation of high-affinity nicotinic receptors in the smoker's brain. To address the molecular mechanism of upregulation, we transfected HEK293 cells with human α4β2 receptors and traced the subunits throughout their intracellular biosynthesis, using metabolic labeling and immunoprecipitation techniques. We show that high-mannose glycosylated subunits mature and assemble into pentamers in the endoplasmic reticulum and that only pentameric receptors reach the cell surface following carbohydrate processing. Nicotine is shown to act inside the cell and to increase the amount of β subunits immunoprecipitated by the conformation-dependent mAb290, indicating that nicotine enhances a critical step in the intracellular maturation of these receptors. This effect, which also takes place at concentrations of nicotine found in the blood of smokers upon expression of α4β2 in SH-SY5Y neuroblastoma cells, may play a crucial role in nicotine addiction and possibly implement a model of neural plasticity.**

## Introduction

In addition to their direct pharmacological action on their specific receptors, many drugs of abuse elicit cellular adaptation following prolonged exposure. These plasticity phenomena described for several G protein-coupled receptors, including the opioid receptor, typically result in receptor internalization followed by downregulation (Roth et al., 1998). In this context, the case of nicotinic acetylcholine receptors (nAChRs) is rather unusual, since long-term exposure to nicotine elicits receptor upregulation in the smoker's brain (Benwell et al., 1988) and in rodent brain (Marks et al., 1983; Schwartz and Kellar, 1983) as well as in cell lines expressing various neuronal nAChRs (Peng et al., 1997; Whiteaker et al., 1998). Upregulation, which corresponds to an increase in high-affinity binding sites for nicotine, in general produces potentiation of the nicotinic response, particularly in cell lines (Buisson and Bertrand, 2001; Gopalakrishnan et al., 1996) and in brain synaptosomes (Nguyen et al., 2004; Rowell and Wonnacott, 1990).

The neuronal nAChRs subject to upregulation are pseudosymmetrical heteropentameric ion channels resulting from the assembly of principal (α2, α3, α4, α6) and complementary (β2, β4) subunits. At the concentrations of nicotine found in the brain of smokers (low micromolar range), the highly expressed α4β2 receptors display the highest level of upregulation (Nguyen et al., 2003). Since receptors containing the β2 subunits are the most important for nicotine self-administration in mice (Picciotto et al., 1998), it is likely that their upregulation contributes to the long-term effect of chronic nicotine and potentially to nicotine addiction (Buisson and Bertrand, 2002). Along with other factors, upregulation may contribute to nicotine sensitization, since both phenomena take place with similar kinetics (Marks et al., 1983).

Since nicotine is known to penetrate the cell membrane (Whiteaker et al., 1998), the localization of its site of action for upregulation, inside the cell or at the cell surface, remains a debated issue. In previous work (Sallette et al., 2004), we identified a protein microdomain that controls the differences of upregulation noticed between β2 and β4 containing receptors. This microdomain is located at the subunit interface, in close contact with the ligand binding site. In spite of this molecular identification, little is known about the cellular mechanisms underlying nicotine upregulation. In vivo studies in both rodents and cell lines have shown no change in mRNA levels following upregulation, pointing to a posttranscriptional effect of nicotine. Many studies were attempted to elucidate the mechanisms by which nicotine upregulates various combinations of nAChRs reconstituted in cell lines and in the *Xenopus* oocytes, leading to a wide range of hypotheses, in particular: (1) a role of nAChR desensitization (Fenster et al., 1999), (2) a decrease of the turnover rate of already assembled surface receptors (Peng et al., 1994), followed by an increased internalization of the receptors (Peng et al., 1997), (3) a maturational role of nicotine that promotes subunit assembly (Wang et al., 1998), or (4) an isomerization of low-affinity surface receptors into high-affinity receptors (Buisson and Bertrand, 2002).

In order to elucidate at which step nicotine acts, we studied the maturation and trafficking of human α4β2 nAChRs expressed in HEK293 cells using pulse-chase metabolic labeling, subunit-specific immunoprecipitation, and glycosydases digestions. Our results show that nicotine acts intracellularly on early maturational steps of ER-located species. A similar intracellular effect of nicotine on early maturational steps is also observed in α4β2 transfected SH-SY5Y human neuroblastoma cells at concentrations of nicotine found in the blood of smokers, further supporting that this mechanism contributes to nAChR upregulation in smokers.

*Correspondence: changeux@pasteur.fr (J.-P.C.); pjcorrin@pasteur.fr (P.J.C.)

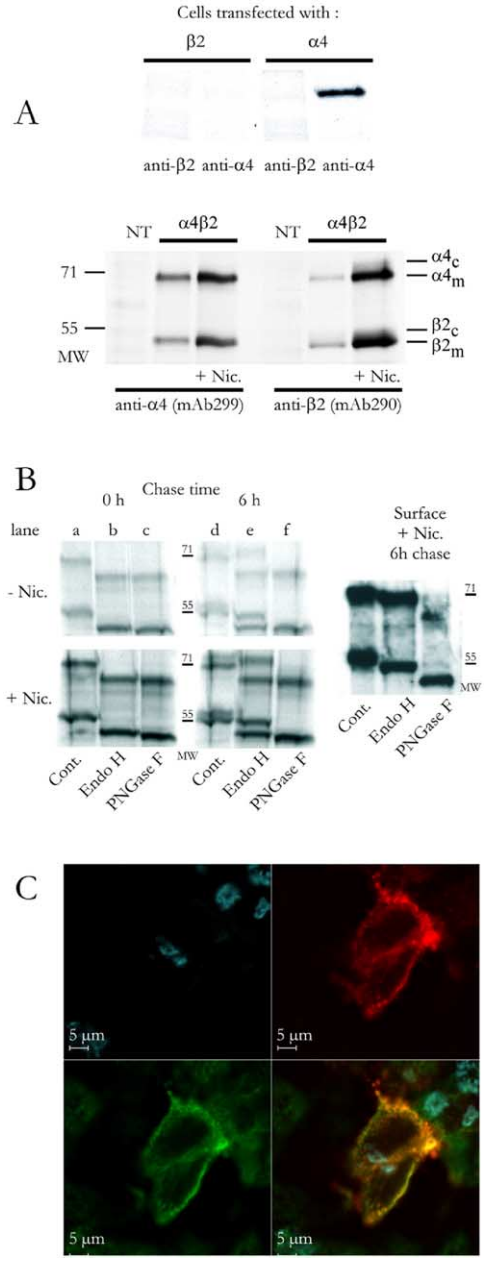


Figure 1. Subunit Processing within HEK293 Cells

(A) Specificity of mAb299 and mAb290 antibodies. (Upper panel) α4 or β2 transfected cells metabolically labeled for 3 hr and immunoprecipitated with mAb299 or mAb290 as indicated, fractionated on a 7% SDS-polyacrylamide gel, and visualized by autoradiography. (Lower panel) Similar experiments on nontransfected (NT) and α4β2 transfected cells, in control (without nicotine) or 1 mM nicotine conditions (+Nic).

(B) Glycosylation state of the α4m, α4c, β2m, and β2c species. Control (–Nic) or 1 mM nicotine upregulated (+Nic) α4β2 transfected cells metabolically labeled for 30 min and chased for 6 hr (lanes d–f) or not (lanes a–c), followed by mAb290 immunoprecipitation, digestion by Endoglycosydase-H (lanes b and e) or by PNGase-F (lanes c and f), running on 7% SDS-polyacrylamide gel and visualization by autoradiography. (Right panel) Surface receptors of α4β2 transfected cells upregulated with 1 mM nicotine were labeled with sulfo-NHS-biotine, immunoprecipitated by mAb290, digested by Endoglycosydase-H or by PNGase-F, run on 7% SDS-polyacrylamide gel, and visualized by immunoblotting with peroxydase-conjugated extravidine.

(C) immunofluorescence imaging in HEK293 cells. Images show a typical HEK cell transfected with α4, β2, and pECFP-Golgi. The Golgi apparatus was visualized by the cyan fluorescence (upper left panel), the β2 subunits by the red fluorescence (upper right panel), and the ER by the green fluorescence (lower left panel). The overlay of the three colors in the lower right panel shows strong colocalization between β2 and the ER (yellow color).

## Results

### Anti-α4 mAb299 and anti-β2 mAb290 Antibodies Display Different Patterns of Subunit Recognition

We expressed the human α4 and β2 subunits by transient transfection in HEK293 cells followed by metabolic labeling. nAChRs were then solubilized with a mixture of lubrol/phosphatidylcholine (Green and Claudio, 1993) and immunoprecipitated with the commercially available anti-α4 mAb299 and anti-β2 mAb290 antibodies (Lindstrom, 1996; Whiting and Lindstrom, 1988). We confirmed their high specificity, but also revealed unexpected patterns of subunit recognition (Figure 1A).

First, mAb299 immunoprecipitated the α4 subunit either when α4 was expressed alone or when expressed together with the β2 subunit. In contrast, mAb290 recognized the β2 subunit only when β2 was expressed with the α4 subunit. In this latter condition, efficient coimmunoprecipitation was observed between α4 and β2, indicating that hetero-oligomerization had occurred after 3 hr of metabolic labeling. Thus, hetero-oligomerization of β2 with α4 is required for the interaction of mAb290 with β2, but not for the interaction of mAb299 with α4.

Second, with α4β2 transfected cells, the α4 and β2 subunit coimmunoprecipitated by mAb290 appeared both as double bands, with the major bands corresponding to those immunoprecipitated by mAb299 (called $\alpha4_m$ and $\beta2_m$, respectively), and minor bands of slightly higher molecular weight (called $\alpha4_c$ and $\beta2_c$, respectively). The apparent molecular weights for $\alpha4_m$, $\beta2_m$, $\alpha4_c$, and $\beta2_c$ estimated on gels were 70, 51, 74, and 54 kDa, respectively.

### Complex Oligosaccharide Glycosylation and Surface Export of the α4β2 Receptors

We then tested the possibility that the different migration profiles correspond to different glycosylation states of the α4 and β2 subunits. Since different glycosylation states typically appear sequentially in the course of the maturation process, we metabolically labeled α4β2 transfected cells for 30 min, followed by a chase period of either 0 or 6 hr. After immunoprecipitation by mAb290, we performed digestions with PNGase-F, which reacts with glycoproteins by eliminating all carbohydrates from N-linked glycosylations, and Endo-H, which reacts with proteins carrying high-mannose carbohydrates (Kornfeld and Kornfeld, 1985). Figure 1B shows that at 0 hr chase, only $\alpha4_m$ and $\beta2_m$ bands are immunoprecipitated (lane a), whereas at 6 hr chase, $\alpha4_c$ and $\beta2_c$ bands are in addition present (lane

d) and correspond to approximatively 40% of the immunoprecipitated material. This suggests that the $\alpha4_m$ and $\beta2_m$ bands are converted into the $\alpha4_c$ and $\beta2_c$ bands in the course of subunit processing.

At 0 hr chase, the digestion profiles of $\alpha4_m$ and $\beta2_m$ by Endo-H and PNGase-F were similar (lanes b and c), with a quantitative conversion into nonglycosylated bands at apparent molecular weights of 64 and 46 kDa, respectively, corresponding to fully deglycosylated subunits, as verified by growing the cells in the presence of tunicamycine followed by immunoprecipitation with mAb 290 (data not shown). These bands fitted reasonably well with the calculated molecular weight from the protein sequence, with 70 kDa for $\alpha4$ (627 amino acids) and 57 kDa for $\beta2$ (502 amino acids). This indicates that these subunit species carry only high-mannose carbohydrates. After 6 hr chase, the $\alpha4_c$ and $\beta2_c$ bands were completely digested by PNGase-F (lane f), but partially resistant to Endo-H treatment (lane e), with intermediate apparent molecular weights of 71 and 50 kDa, respectively, thus showing that $\alpha4_c$ and $\beta2_c$ bands carry a mixture of high mannose and complex type carbohydrates.

The protein sequences of $\alpha4$ and $\beta2$ reveal, respectively, three (at positions 38, 88, and 155) and two (at position 33 and 150) putative N-glycosylation sites (Monteggia et al., 1995). Interestingly, Endo-H treatment reduced the apparent molecular weight by 3–4 kDa on both $\alpha4_c$ and $\beta2_c$, and PNGase-F removed 10 and 8 kDa, respectively, suggesting that one putative glycosylation site in both $\alpha4$ and $\beta2$ remains of the high-mannose type, the remaining two (for $\alpha4$) and one (for $\beta2$) being further processed to complex carbohydrate.

These observations suggest that the $\alpha4_m$ and $\beta2_m$ correspond to subunits located in the proximal secretory pathway, from the ER to medial Golgi, while $\alpha4_c$ and $\beta2_c$ have escaped from these compartments and have undergone trimming and complex oligosaccharide glycosylations in the medial-Golgi. Such a scheme predicts that surface $\alpha4\beta2$ should be composed only of $\alpha4_c$ and $\beta2_c$ subunits. To test this possibility, we specifically labeled surface receptors by subjecting the $\alpha4\beta2$ transected cells to a membrane impermeant biotinylation reagent (sulfo-NHS-biotine), followed by an immunoprecipitation with mAb290 and immunoblotting with peroxydase-conjugated extravidine. Differential digestion by Endo-H (Figure 1B) or by PNGase-F showed that the entire population of surface nAChRs is made of partially Endo-H-resistant subunits.

To investigate the cellular location of the $\beta2$ subunits within the cells, we performed immunofluorescence imaging experiments. HEK293 cells were transfected with the $\alpha4$ and $\beta2$ subunits, along with a pECFP-Golgi protein, which contains the targeting sequence from human $\beta1$,4-galactosyltransferase. After fixation of the cells, the $\beta2$ subunit was labeled by mAb290, and the ER-associated protein disulfide isomerase was labeled using a primary antibody. Figure 1C shows that the majority of the $\beta2$ subunits colocalized with the ER marker, whereas no or weak colocalization was observed with the Golgi protein. These data show that the majority of $\beta2$ subunits are distributed within the ER.

Altogether, our data indicate that within 30 min after metabolic labeling, subunits are present in their high-mannose form and are thus probably located in the ER. Efficient coimmunoprecipitation between $\alpha4$ and $\beta2$ is already observed at this stage, pointing to the presence of hetero-oligomers. At 6 hr chase, a significant fraction of subunits carrying complex oligosaccharides is present in the whole-cell population, suggesting that they belong to receptors that have escaped the ER and have been processed in the Golgi apparatus. Only subunits carrying complex oligosaccharides are found at the cell surface.

### Pentameric Assembly Is Required for Receptor Complex Glycosylations and Surface Export

Sedimentation analysis of nonradioactive lubrol/phosphatidylcholine-solubilized $\alpha4\beta2$ receptors followed by measurement of [$^3$H]-epibatidine binding on each fraction of the gradient (Figure 2A) shows the species displaying high affinity for [$^3$H]-epibatidine sediment as a peak that corresponds to pentameric receptor, as previously reported for Triton X-100 solubilized human $\alpha4\beta2$ receptors (Nelson et al., 2003). However, in contrast to Triton X-100 solubilized receptors that give a narrow peak (confirmed in the present study, data not shown), the decrease of this peak at the high sedimentation coefficients is relatively slow, indicating that higher molecular weight species potentially also bind [$^3$H]-epibatidine.

The oligomeric distribution of the different glycosylation states of $\alpha4$ and $\beta2$ subunits was assessed by metabolically labeling $\alpha4\beta2$ cells for 3 hr and immunoprecipitating each fraction of the gradient with mAb290. Figure 2B shows that $\alpha4_c$ and $\beta2_c$ both exhibited a single peak centered at the pentamer level, whereas $\alpha4_m$ and $\beta2_m$ species were more widely distributed, with around 60% of the total amount of each subunit sedimenting at a peak corresponding to the pentameric form. The remaining 40% were spread in all the fractions corresponding to higher sedimentation coefficients, indicating the presence of a heterogeneous population of oligomers containing more than five subunits.

These results show that subunit pentamerization occurs before carbohydrate trimming and processing, most probably within the ER. The higher-order oligomer population found in the ER appeared heterogeneous, but at least a subpopulation bound [$^3$H]-epibatidine with high affinity. These species may constitute either intermediate oligomers in the course of the maturation process, incorrectly assembled oligomers that would no longer give rise to mature receptors and be eventually degraded, or small aggregates resulting from prolonged solubilization in lubrol/phosphatidylcholine. In this latter case, it is noteworthy that such species are not observed for subunits harboring complex oligosaccharides, indicating that such aggregation would involve relatively immature subunits. Interestingly, subunits harboring complex oligosaccharides were only integrated in pentameric receptors, suggesting that correct pentamerization is a requirement to escape the quality control of the ER.

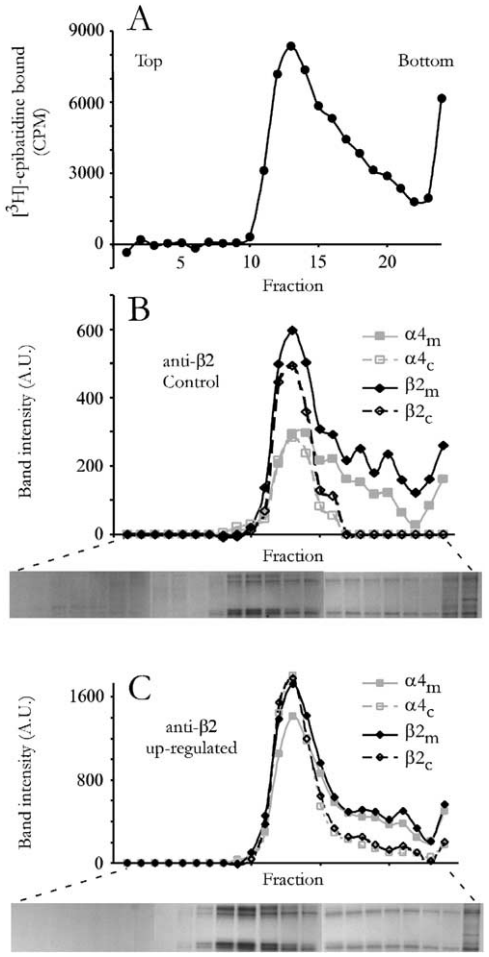


Figure 2. Nature of the Oligomeric Species in HEK293 Cells

(A) Solubilized receptors from $\alpha4\beta2$ transfected cells were run on a 3%–30% sucrose gradient, and [$^3$H]-epibatidine binding was measured for each fraction.

(B and C) Control (panel B) or 1 mM nicotine upregulated (panel C) $\alpha4\beta2$ transfected cells metabolically labeled for 3 hr, solubilized, and ran on a 3%–30% sucrose gradient. Each fraction was immunoprecipitated by mAb290 and fractionated on 7% SDS-polyacrylamide gel. For each gradient, the bottom panel shows the gels visualized by autoradiography, and the upper panel shows its quantification by scanning densitometry. $\alpha4$ and $\beta2$ species are represented by gray squares and black diamonds, respectively, whereas high-mannose and complex oligosaccharide carrying species are drawn with full and dashed lines, respectively.

### Upregulation by Nicotine: Parallel Increase in High-Affinity Binding Site and in Immunoprecipitation of the Different Subunit Species

As a next step, we investigated the effect of chronic nicotine on these cellular processes. When cells are grown for 24 hr in the presence of 1 mM nicotine, upregulation (measured as the increase of the number of high-affinity binding sites for the agonist [$^3$H]-epibatidine as compared to control condition without nicotine) was concentration dependent (Figure 3A) with a sigmoid shape ($EC_{50}$ around 0.1 $\mu$M, Hill number [nH] = 1) and a maximal upregulation of 2.44 ± 0.11-fold. When cells were cultured for only 3 hr in the presence of nicotine, a procedure that more closely replicates immunoprecipitation experiments (see below), the concentration-dependence curve shifted to higher concentrations, with an $EC_{50}$ around 1 $\mu$M (nH = 1) but a comparable maximal amplitude (2.05 ± 0.25-fold). This indicates that, within 3 hr, the steady state of upregulation is not reached at submaximal concentrations. Finally, we evaluated the fraction of surface versus intracellular number of binding sites by taking advantage of the high membrane permeability for epibatidine and of the membrane impermeability of the agonist carbamylcholine during the 30 min binding assay (Whiteaker et al., 1998). Figure 3A′ shows that, in control and upregulated conditions, carbamylcholine displaced 13.4% ± 1.2% and 19.7% ± 7.0% of the [$^3$H]-epibatidine binding sites, respectively, indicating that (1) around 85% of the sites were not accessible to carbamylcholine and were therefore intracellular in both conditions and that (2) nicotine did not dramatically change the proportion of surface versus intracellular binding sites.

The changes in the amount of immunoprecipitated subunits associated to "upregulation in binding" was assessed by performing mAb299 or mAb290 immunoprecipitations of solubilized nAChRs from cells upregulated by increasing concentrations of nicotine. In all the following immunoprecipitation experiments, nicotine and nicotinic ligands were added to the culture medium 24 hr before metabolic labeling and remained at the same concentration during methionine deprivation, metabolic labeling, and chase step. In the present experiments, we selected a 3 hr metabolic labeling with no chase period. A roughly linear concentration-dependent increase in the amount of immunoprecipitated subunits was observed with both antibodies (Figures 3B and 3C), as a function of log([nicotine]), independent of the antibody used or the species considered. In particular, no significant change was observed upon nicotine treatment in (1) coimmunoprecipitation, since both the $\alpha4_m/\beta2_m$ and $\alpha4_c/\beta2_c$ ratios remained stable at the different concentrations of nicotine (0.61 ± 0.07 and 0.99 ± 0.18 for $\alpha4_m/\beta2_m$ in mAb290 and mAb299 immunoprecipitations, respectively, and 0.54 ± 0.11 for $\alpha4_c/\beta2_c$ in mAb290 immunoprecipitation) or (2) complex glycosylated versus high-mannose subunits (0.50 ± 0.06 and 0.44 ± 0.07 for $\beta2_c/\beta2_m$ and $\alpha4_c/\alpha4_m$, respectively, in mAb290 immunoprecipitation experiments, Figure 3B′).

Therefore, upregulation in binding, corresponding to an increased number of oligomers displaying high affinity for epibatidine, is concomitant to an "upregulation in immunoprecipitation," corresponding to an increased number of $\alpha4\beta2$ hetero-oligomers immunoprecipitated by both mAb290 and mAb299. It is noteworthy that both processes are observable at a nicotine concentration as low as 10 nM. However, significant differences were found in the concentration-dependence curves: (1) the increase in binding site was maximal at 10 $\mu$M nicotine concentration, whereas the amount of immunoprecipitated subunits continued to increase in an apparent linear manner at 100 $\mu$M and 1 mM; (2) the maximal increase in binding sites was 2.5-fold, as compared to the increase in subunit immunoprecipitation that reached 3- to 4-fold. These differences are probably due to the fact that different populations of receptor subunits are observed in both experiments: binding

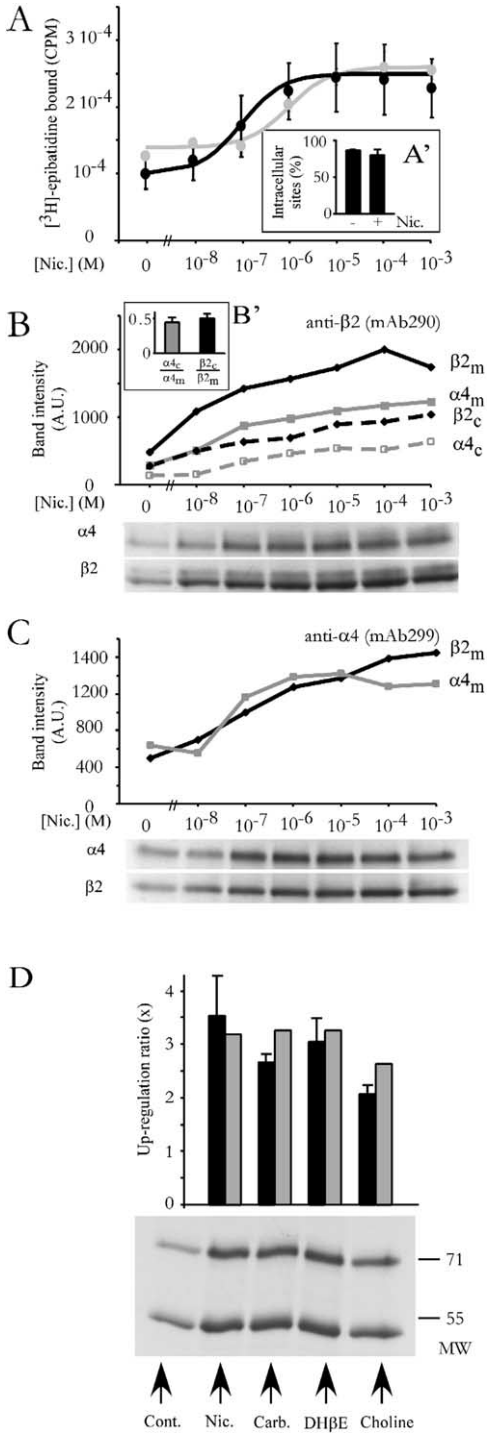


Figure 3. Pharmacology of Upregulation in Binding and in Immunoprecipitation in HEK293 Cells

(A) [$^3$H]-epibatidine binding dose upregulation curve after 3 (gray) and 24 hr (black) nicotine incubation. The percentage of intracellular versus surface binding sites in upregulated and control conditions, evaluated using carbamylcholine competition (at 1 mM during 30 min), is shown in (A′). Points are the mean of three experiments, and error bars represent standard deviation.

(B and C) Dose upregulation curves performed using $\alpha4\beta2$ transfected cells metabolically labeled for 3 hr, immunoprecipitated by mAb290 (B) or mAb299 (C), and fractionated on 7% SDS-polyacrylamide gel. For each experiment, the bottom panel shows the gel visualized by autoradiography, and the upper panel shows its quantification by scanning densitometry. $\alpha4$ and $\beta2$ species are represented by gray squares and black diamonds respectively, whereas high-mannose and complex oligosaccharide carrying species are drawn with full and dashed lines, respectively. The global mean ratio of complex versus high-mannose carbohydrate carrying subunits ratios for $\alpha4$ (gray) and $\beta2$ (black) is shown in (B′).

(D) $\alpha4\beta2$ transfected cells were upregulated by either 1 mM nicotine, 1 mM carbamylcholine, 100 μM DHβE, or 1 mM choline. These compounds were continuously present during a 24 hr period in the culture medium and during the following 30 min of metabolic labeling and 45 min of chase. Receptors were immunoprecipitated by mAb290 and visualized by autoradiography (lower panel) followed by quantification by scanning densitometry (gray bars in the upper panel, which represent the increase in the $\alpha4$ band intensity as compared to control conditions). In parallel, the upregulation ratios of the [$^3$H]-epibatidine binding sites were measured on cells upregulated under the same conditions (black bars, which represent the mean of three independent experiments, error bars represent standard deviation.).

studies measure the entire receptor population present in the cells, whereas immunoprecipitation experiments reveal only subunits that have been synthesized during the 3 hr of metabolic labeling.

### Upregulation Is Concomitant with a Functional Potentiation of the Electrophysiological Response

We recorded the electrophysiological response of $\alpha4\beta2$ transfected HEK293 cells when cells were grown in control medium or after 24 hr upregulation by 1 μM and 1 mM nicotine. Figure 4 shows typical current traces when receptors were rinsed for 1 hr with nicotine-free medium and then activated by two concentrations of ACh, one below its $EC_{50}$ (at 30 μM) and one at a saturating concentration (1 mM). Activation by 1 mM ACh illustrates that prolonged exposure of nicotine at 1 μM and 1 mM induces a potentiation of the response, which reaches respectively 1.5- and 1.7-fold (Figure 4B). The potentiation is associated with significant changes in the receptor properties: (1) the ratio I(30 μM)/I(1 mM) increased from 0.30 to 0.38 and 0.39 in control, 1 μM and 1 mM upregulated conditions, respectively, indicating a change in ACh $EC_{50}$ (Figure 4B); (2) upregulated receptors display significantly slower desensitization kinetics. Fitting the desensitization component of the traces with a monoexponential yielded time constants of 430 ± 80 and 900 ± 200 ms for control and 1 mM upregulated conditions, respectively. Thus, upregulated receptors are functional, since the ratio of upregulation in binding (2.4-fold) and of functional potentiation in electrophysiology (1.7-fold) are comparable. Moreover, the functional potentiation is associated with a decreased $EC_{50}$ for ACh and slower desensitization kinetics, as previously described for human $\alpha4\beta2$ receptors stably expressed in HEK293 cells (Buisson and Bertrand, 2001).

### Nicotine Upregulation in Immunoprecipitation Occurs Intracellularly on High-Mannose Glycosylated Subunits

To investigate in more detail which subunit species are upregulated by nicotine, we subjected 1 mM nicotine

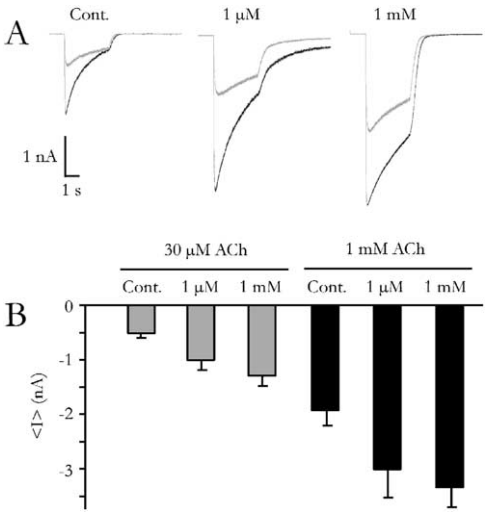


Figure 4. Functional Potentiation of $\alpha4\beta2$ Receptors in HEK293 Cells

(A) typical trace currents evoked by a 3s application of ACh at 30 μM (gray traces) and 1 mM (black traces) on $\alpha4\beta2$ transfected cells in control condition and after 24 hr upregulation by 1 μM and 1 mM nicotine. Note that the kinetics of desensitization is decreased in upregulated conditions.

(B) Mean currents evoked by these ACh concentrations in control, 1 μM, and 1 mM nicotine upregulated cells (each value represents the mean of 13 cells, error bars represent standard error of mean), illustrating the functional potentiation of 1 mM ACh-evoked currents and that 30 μM ACh-evoked currents are more potentiated than 1 mM ACh-evoked currents, indicative of a decrease of the ACh $EC_{50}$.

upregulated $\alpha4\beta2$ expressing cells to immunoprecipitation experiments, followed either by digestions with glycosidases or sucrose gradient sedimentation analysis.

Figure 1B shows that similar patterns of Endo-H/PNGase-F digestion were observed between control and upregulated cells (lanes b and c). After 30 min metabolic labeling with no chase period, no complex glycosylated bands were formed, and nicotine increased the amount of high-mannose subunits by about 3-fold. At the 6 hr chase period (lane d), high-mannose and complex oligosaccharide subunits were increased in a similar manner by nicotine treatment, suggesting that nicotine did not significantly alter the subsequent processes of trimming and complex oligosaccharide glycosylations.

Sucrose gradient analysis revealed that the oligomeric distribution is not qualitatively altered by the presence of chronic nicotine (Figure 2C). The subunits carrying complex oligosaccharides remained completely associated in pentamers, and the ratio of pentameric versus higher oligomeric states was not significantly changed for the high-mannose population. Nicotine action resulted in a global increase (around 3-fold) in the amount of immunoprecipitated proteins, regardless of the type of oligomer.

Altogether, the main consequence of chronic nicotine is to increase the intensity of the high-mannose bands as early as 30 min after protein synthesis, thus providing an unambiguous demonstration of an intracellular action of nicotine on the early step of subunit maturation.

### Pharmacology of Upregulation of Immunoprecipitated Material

We tested the agonists nicotine (1 μM) and carbamylcholine (1 mM) and the antagonist dihydro-β-erythroïdine DHβE (100 μM)—all reported to elicit upregulation—and choline (1 mM), which is the precursor in the biosynthesis of acetylcholine. Figure 3D shows that a good correlation exists between upregulation in binding sites and in immunoprecipitation by mAb290 of the high-mannose species: 3.5 and 3.2 for nicotine upregulation in binding sites and immunoprecipitation, respectively, 2.7 and 3.3 for carbamylcholine, 3.1 and 3.3 for DHβE, and 2.1 and 2.6 for choline. It is noteworthy that the compounds were in all cases added to the culture medium 24 hr before performing the metabolic labeling (30 min) and the chase (45 min). This procedure was selected in order to optimize the intensity of the subunits carrying high-mannose carbohydrates as compared to those carrying complex carbohydrates (see below). These data demonstrate that the various nicotinic effectors tested produce upregulation by an intracellular action. Therefore, even the weakly membrane-permeable compound carbamylcholine, which does not enter the cell to significant extent during the 30 min currently used for binding experiments, does enter the cell after 24 hr incubation to a sufficient extent to produce intracellular upregulation.

### Dynamic Study of Nicotine Upregulation Reveals an Effect on the Early Steps of Subunit Maturation

Time-resolved investigation of chronic nicotine action on the different stages of subunit processing was performed by pulse-chase experiments after 30 min metabolic labeling (Figure 5).

In control condition, the high-mannose bands were most intense at 0 hr chase and decreased with apparent half-life times ($t_{1/2}$) around 8 and 6 hr in mAb290 and mAb299 immunoprecipitation experiments, respectively (Figures 5A and 5C). The subunits carrying complex oligosaccharides were absent at no chase, as already observed (Figure 1B). mAb290 immunoprecipitated increasing amounts of $\alpha4_c$ and $\beta2_c$ during the first 3 hr chase, followed by a slow decrease. Assuming that mAb290 recognized the high-mannose and complex carbohydrate species with similar affinities, these data suggest that around 60% of the $\alpha4_m/\beta2_m$ present at 0 hr chase are converted into $\alpha4_c/\beta2_c$ species in the course of subunit processing, the remaining subunits being degraded by the cellular machinery.

In 1 mM nicotine upregulated conditions, the level of immunoprecipitated subunits was strongly increased (Figures 5B and 5D). At 0 hr chase, the high-mannose bands were significantly upregulated as compared to control condition (Figures 5E, 5F, 5H, and 5I), and continued to increase during the first 45 min of chase in the case of mAb290 (50% increase) to reach 1.8/2.3 and 5.3/3.4 upregulation of the $\alpha4_m/\beta2_m$ species in mAb299 and mAb290 experiments, respectively. 45 min after chase, all bands decreased following a biexponential decay with a main contribution (around 90%) of a half-

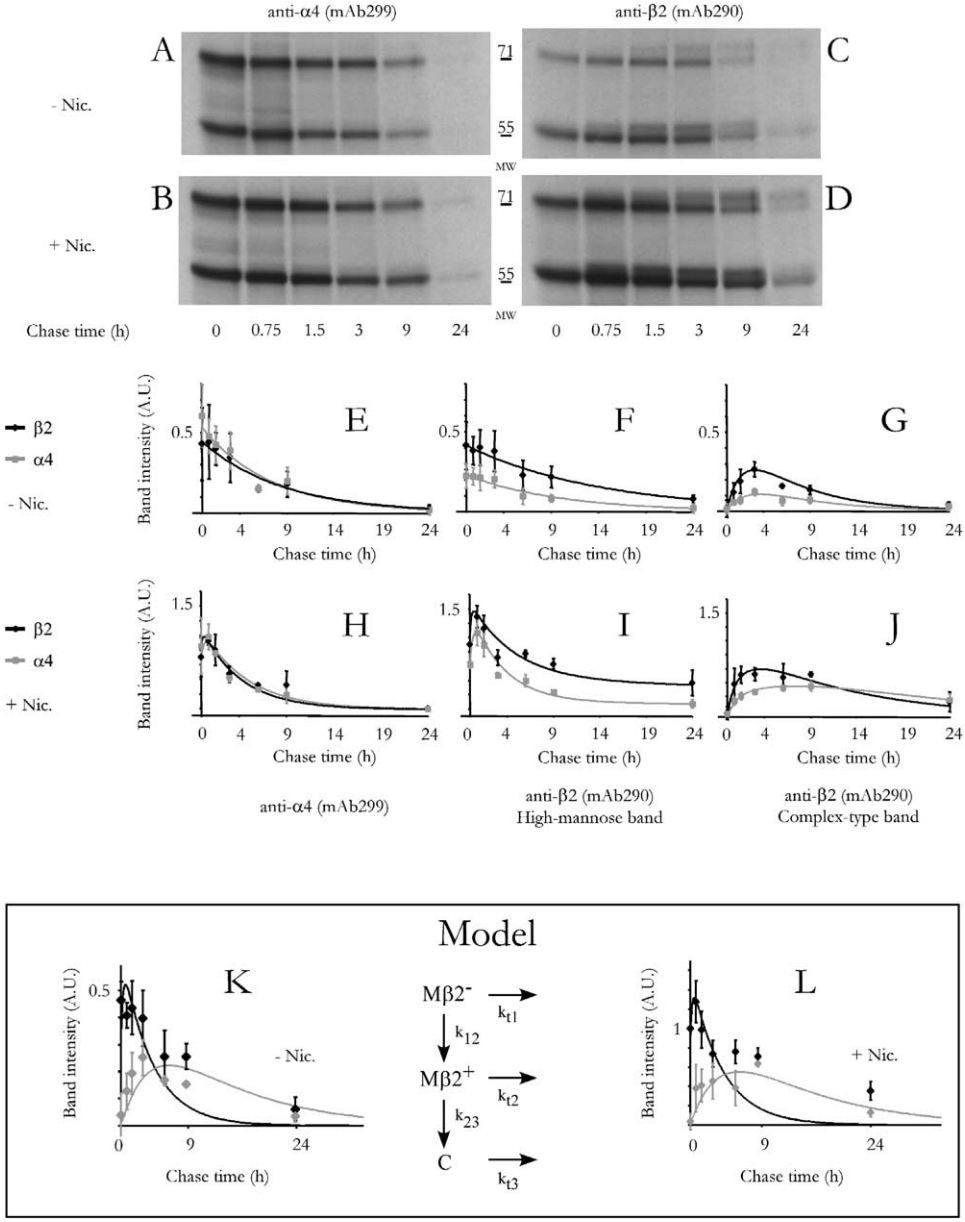


Figure 5. Kinetics of Appearance and Turnover of the Different Species in HEK293 Cells

Control (A and C) or 1 mM nicotine upregulated (B and D) α4β2 transfected cells were labeled for 30 min, chased at various times, immunoprecipitated with mAb299 or mAb290, run on 7% SDS-polyacrylamide gel, and visualized by autoradiography ([A] and [B] for mAb 299, quantified in [E] and [H], and panel [C] and [D] for mAb290, the high-mannose bands being quantified in [F] and [I] and the complex oligosaccharide carrying subunits being quantified in [G] and [J]). α4 and β2 species are represented by gray squares and black diamonds, respectively. Experimental points were fitted by empirical multiexponentials (E–J). Panels (A)–(D) show a typical experiment, and panels (E)–(J) represent the mean of three independent experiments, error bars represent standard deviation. (K and L) Pulse-chase experiments of the mAb290 immunoprecipitated β2 subunit species (experimental points from panels [F], [G], [I], and [J]) and their fits according to the two-step maturational model.

time around 4 hr. The kinetics of formation and turn over of $\alpha 4_c$ and $\beta 2_c$ were not significantly altered, but their amount was upregulated by around 3-fold as compared to control conditions (Figures 5G and 5J).

Altogether, these data show a dramatic effect of nicotine on the early step of subunit maturation: (1) the increase in mAb290 and mAb299 immunoprecipitation was observed as soon as 0 hr chase, indicating an early action during the 30 min of radioactive subunit synthesis, and (2) the increase in subunit immunoprecipitation elicited by nicotine 45 min after the end of radioactive subunit synthesis indicated that at 0 chase a subpopulation of the subunits were not immunoprecipitated by mAb290 and that nicotine converted at least a fraction of this subpopulation into a conformation compatible with mAb290 recognition. Indeed, we showed that het-

ero-oligomerization of the β2 subunit was required for mAb290 antibody recognition, indicating that newly synthesized β2 subunits are not recognized by mAb290.

To tentatively assess the contribution of the maturational process in upregulation, we developed a simplified two-step sequential model presented in Figure 5. It postulates that newly synthesized high-mannose β2 subunits are in an immature conformation not recognized by mAb290, called Mβ2$^{-}$. In the course of maturation, Mβ2$^{-}$ are converted to Mβ2$^{+}$ (high-mannose β2 recognized by mAb290) and then to C (complex carbohydrate β2), according to first-order rate constants. Each species is degradated according to first-order kinetics. During the 30 min of metabolic labeling, Mβ2$^{-}$ species are synthesized according to a linear time function "at." Fitting kinetic data (Figures 5K and 5L) according to this model (described in the Supplemental Data available with this article online) yielded a reasonable set of parameters: in both control and upregulated conditions, the a, $k_{23}$, $k_{t1}$, $k_{t2}$, and $k_{t3}$ were identical and equal to $2 \times 10^{-1}$, $2.5 \times 10^{-3}$, $5 \times 10^{-2}$, $1.5 \times 10^{-3}$, and $1.5 \times 10^{-3}$ min$^{-1}$, respectively. Only the $k_{12}$ constant changed, from $6 \times 10^{-3}$ to $18 \times 10^{-3}$ min$^{-1}$, in control and upregulated conditions, respectively. This illustrates that a single change of the $k_{12}$ constant, which represents the rate of conversion of Mβ2$^{-}$ into Mβ2$^{+}$, is sufficient to reasonably account for the effect of nicotine on upregulation. Whereas maturation is clearly a multistep process, the model states that nicotine promotes early-step maturation of subunits that would otherwise be degraded.

### Nicotine Promotes Intracellular Subunit Maturation in SH-SY5Y Neuroblastoma Cells

To investigate the contribution of this mechanism in neuronal cell lines, we used transiently transfected human α4β2 SH-SY5Y human neuroblastoma cells. These cells resemble human fetal sympathetic neurons grown in primary culture and express mRNAs for α3, α5, α7, β2, and β4 subunits (Lukas et al., 1993) and functional α7 and α3 containing nAChRs, the latter receptors being strongly upregulated by chronic nicotine (Peng et al., 1997). We first tried to metabolically label and immunoprecipitate with mAb290 the endogenous β2 subunits from these cells, but found no specific bands, indicating that the amount of endogenous β2 subunits were too low to be detected by this technique. We thus transfected these cells with the α4 and β2 subunits using the calcium phosphate procedure. [$^{3}$H]-epibatidine binding shows that nontransfected cells carry 3.2 ± 0.4 fmol/dish high-affinity binding sites, and this value raises to 4.9 ± 2.0 and 25.0 ± 13 upon upregulation by 1 μM and 1 mM nicotine, respectively. Upon transfection, high-affinity binding site increased, with 89.3 ± 8.0, 162.5 ± 5.2, and 271 ± 8.9 fmol/dish in control, 1 μM and 1 mM upregulated conditions, respectively. It is noteworthy that the transfected HEK293 cells express around 10-fold more binding sites than transfected SH-SY5Y.

In mAb290 immunoprecipitation experiments, metabolic labeling for 30 min followed by different chase periods indicates that the processing of the α4 and β2 subunit were similar in SH-SY5Y and HEK 293 cells. At 0 hr chase, the α4 and β2 subunits were present only in their high-mannose form and were quantitatively digested by EndoH and PNGase-F, whereas at 6 hr chase, subunits carrying complex carbohydrates appeared and were partially resistant to EndoH treatment (Figure 6A, upper panels). The apparent molecular weight of all glycosylation states for both subunits were similar in SH-SY5Y and HEK293 cells. Pulse-chase experiments further showed that the kinetics of high-mannose species turnover were similar between both cell lines (Figure 6A, lower panel). Incubation of the cells with 1 μM and 1 mM nicotine resulted in a strong increase in the amount of immunoprecipitated subunits. Because of the low level of transfected subunits in the neuroblastoma cells, their quantification was difficult, and the complex olisaccharide bands were barely visible in some cases. To limit the variability between experimental points, green fluorescent protein was used as an internal standard for the transfection and sample processing efficiency. Thus, in these pulse-chase experiments, GFP was coexpressed along with the α4 and β2 subunits, and proteins were independently immunoprecipitated with the anti-GFP and mAb290 antibodies before loading on the gel. Quantification of the α4 and β2 bands normalized to the GFP band clearly show that nicotine at 1 μM and 1 mM significantly upregulates the subunits at all chase times (Figure 6B, with upregulation ranging from 1.5- to 3.5-fold), especially at 0 and 45 min chase, where most subunits carry high-mannose carbohydrates. Finaly, we investigated the cellular location of the transfected β2 subunit within the SH-SY5Y neuroblastoma cells and found that they colocalize in majority with the ER, in a similar way to what is found in HEK293 cells (Figure 6C).

These data show that the intracellular increase of the high-mannose species observed upon transfection in HEK293 cells also occurs in SH-SY5Y neuroblastoma cells, at low micromolar concentrations of nicotine, indicating that similar mechanisms of upregulation are taking place in both cell lines.

## Discussion

### Maturation and Trafficking of α4β2 Receptors

Our results dissect some elementary steps of neuronal nicotinic receptor maturation and surface export. Subunits are initially synthesized as core-glycosylated high-mannose glycoproteins. This type of carbohydrate is known to be inserted cotraductionally and to be characteristic of peptides residing in the proximal secretory pathway, from the ER to medial Golgi (Ellgaard and Helenius, 2003). Within this compartment, the α4 and β2 subunits rapidly hetero-oligomerize, a step during which the β2 subunit undergoes a conformational maturation that allows interaction with mAb290. These processes result in the generation of a mixed population of pentameric oligomers and of a heterogeneous higher molecular weight oligomer population that probably corresponds either to misfolded entities or to small aggregates formed from immature subunits (Cooper and Millar, 1997).

We also found that only pentameric receptors exit from these compartments, as observed for muscle-type nAChRs (Smith et al., 1987). Pentameric receptors

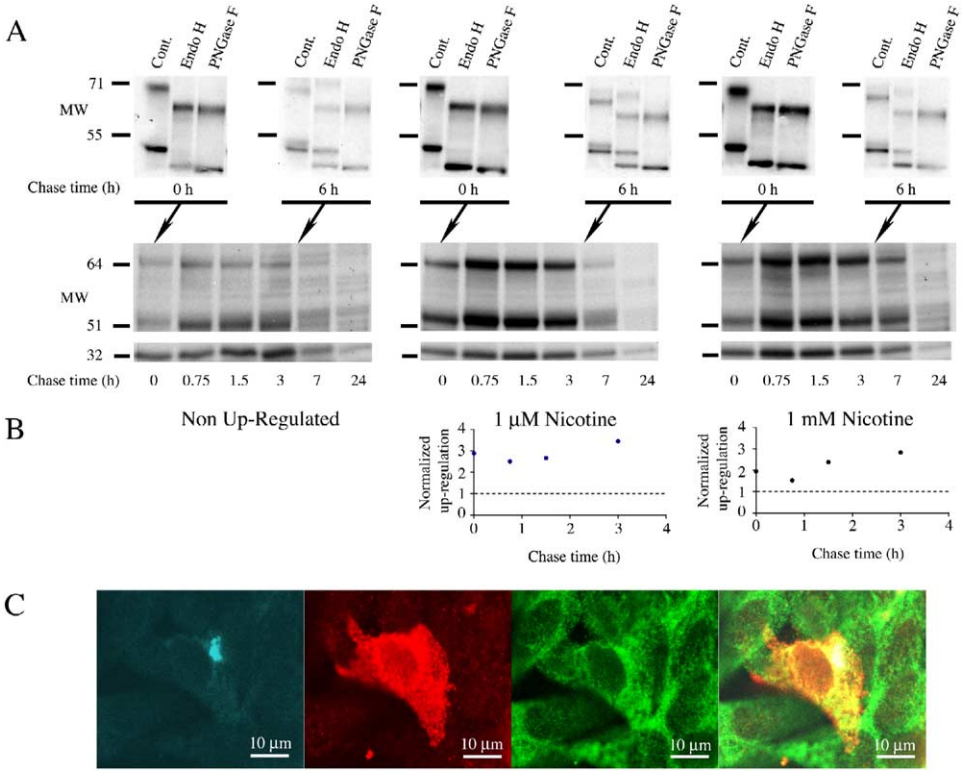


Figure 6. Nicotine Upregulation in α4β2 Transfected SH-SY5Y Neuroblastoma Cell Lines

(A) (Upper panel) Control, 1 μM, and 1 mM nicotine upregulated α4β2 transfected SH-SY5Y neuroblastoma cells were labeled for 30 min and chased for 0 or 6 hr, followed by Endo-H or PNGaseF treatment, mAb290 immunoprecipitation, and 7% SDS-polyacrylamide gel. (Lower panels) More resolved pulse-chase experiments on SH-SY5Y cells tranfected with both α4β2 and GFP, followed by immunoprecipitation with mAb290 and anti-GFP and 10% SDS-polyacrylamide gel (shown is the portion of the gel where α4 and β2 migrate and the portion where GFP [32 kD] migrates).

(B) Quantification of upregulation. For each line, the normalized expression, equal to the sum of the α4 and β2 bands intensity divided by the GFP protein band intensity, was calculated. Each point represents the normalized upregulation, equal to the normalized expression in upregulated condition divided by the normalized expression in control conditions. Points corresponding to long chase periods are not shown because bands were too low to be quantified accurately.

(C) Immunofluorescence imaging in SH-SY5Y cells. Images show a typical cell transfected with α4, β2, and pECFP-Golgi. The Golgi apparatus was visualized by the cyan fluorescence (left panel), the β2 subunits by the red fluorescence (middle left panel), and the ER by the green fluorescence (middle right panel). The overlay of the three colors in the right panel shows strong colocalization between β2 and the ER (yellow color).

are then processed within the secretory pathway where the subunits acquire Endo-H resistance, most likely within the medial-Golgi, to eventually reach the cell surface. This process takes around 3 hr, in agreement with the average process time to produce high-affinity surface muscle-type nAChRs (Merlie and Lindstrom, 1983). Partial EndoH resistance of $\alpha4_c$ and $\beta2_c$ suggested the presence of one high-mannose carbohydrate on these subunits, which may be located in the cys loop, as already shown for the δ nAChR subunit (Strecker et al., 1994). Since the cys loop is known to be hidden in the course of the maturation pathway (Green and Wanamaker, 1997), the concomitant hindrance of this high-mannose glycosylated site could plausibly be one of the conformational signals governing escape from the ER.

We also show that the exit from the ER to medial Golgi compartment is a relatively slow process as compared to the maturation steps. Maturation, as judged by hetero-oligomerization and mAb290 recognition, is nearly completed after 30 min, whereas trafficking and complex oligosaccharide glycosylations require around 3 hr. Therefore, our kinetic data clearly show that exit from the ER is the limiting step within the secretory pathway, pointing to an accumulation of protein within the ER, a feature that is commonly observed for nAChRs expressed in cell lines (Grailhe et al., 2004), in neurons (Nashmi et al., 2003), and in rodent brain (Arroyo-Jimenez et al., 1999). Accordingly, we observed an accumulation of high-affinity binding sites in intracellular compartments (85% inside the cell and 15% at the cell surface) and a strong colocalization of the β2 subunit with the ER by immunofluorescence imaging. Similar values for intracellular nAChR percentages were obtained for other receptors expressed in cell lines (Harkness and Millar, 2002; Peng et al., 1997; Whiteaker et al., 1998).

### Nicotine and Upregulating Ligands Act as Maturational Enhancer

Our dissection offered the possibility to directly assess the action of nicotine on the various cellular processes.

We demonstrate herein an action of nicotine on the early maturation of the subunit protein, since (1) *nicotine acts intracellularly*: nicotine elicits a major increase in the amount of high-mannose oligomers recognized by both mAb290 and mAb299. Since these oligomers are not found at the cell surface, these experiments demonstrate an intracellular action of nicotine, but also of carbamylcholine, DHβE, and choline; (2) *nicotine acts shortly after protein synthesis*: as soon as 30 min after protein synthesis, nicotine elicits a 2-fold increase in the amount of subunit immunoprecipitated by both antibodies; furthermore, nicotine also elicits a major change during the 45 min following the 30 min metabolic labeling, by increasing by 1.5-fold the amount of immunoprecipitation by mAb290; this indicates that, during this period, a fraction of the subunit oligomers are converted into species with a conformation that is recognized by mAb290. The fitting of the dynamic data with a simple sequential two-step model suggests that nicotine acts on a population of subunits/oligomers not recognized by mAb290, which we called "nicotine sensitive precursors," facilitating the conversion of these precursors into species recognized by mAb290, and that display higher metabolic stability.

Thus, the α4β2 receptor matures rather inefficiently, a process that is partly overcome by the action of nicotine during the early steps of the intracellular maturational processes. Nicotine therefore acts as a "maturational enhancer" (Figure 7). This mechanism is similar to the pharmacological rescue of G protein-coupled receptors, initially identified for vasopressin receptor congenital mutations (Morello et al., 2000). It is noteworthy that the inefficient maturation of nAChRs is not only observed in transfected cell lines, but also in native tissues. For example, in the rat brain, the majority of α4 subunits are found inside the cells (Arroyo-Jimenez et al., 1999). A recent paper by Christianson and Green (Christianson and Green, 2004) also shows that the maturation of the muscle-type nAChRs in mouse myotubes is inefficient, since proteasome inhibitors upregulate the number of high-affinity receptors at the cell surface by allowing the processing of subunits that would otherwise be degradated. Thus, inefficient maturation is not restricted to recombinant systems and seems to be a common property of nAChRs.

While the maturational enhancer mechanism is clearly the major cause of upregulation in our experimental paradigm, the present study is not incompatible with other long-term effects of nicotine that were previously reported. First, it is possible that a reduced turnover rate of the receptor makes a minor contribution to upregulation, as previously suggested for α3β2 receptors (Wang et al., 1998), but such a contribution would be too weak to be monitored within the precision of our experiments. Second, upregulation is associated with a change in the functional properties of the receptors (Buisson and Bertrand, 2001), a feature that we confirm by electrophysiological methods. It is thus possible that nicotine also acts on functional surface receptors to displace an equilibrium between low- and high-affinity states of α4β2 receptors, as previously proposed (Buisson and Bertrand, 2001). Still, the maturational enhancer mechanism can account for such a functional alteration, if one assumes that nicotine promotes a particular maturational pathway that would ultimately favor a different receptor state. For instance, an increased proportion of the β subunit within functional pentamers has been shown to be concomitant with α4β2 receptor upregulation (Nelson et al., 2003). We do not observe significant changes in the α/β ratio following upregulation in our immunoprecipitation experiments, but since these experiments examine the entire population of the receptors, alteration of receptor stoichiometries within specific subpopulations cannot be ruled out. Further studies would be required to test these possibilities.

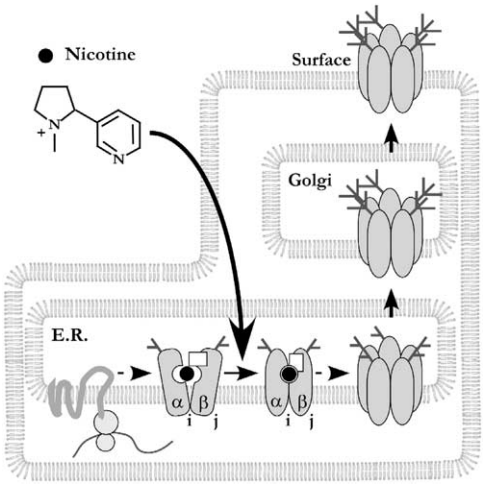


Figure 7. Mechanism of Nicotine Upregulation Inferred from Immunoprecipitation Experiments

Cartoon schematically representing the maturation and trafficking of α4β2 receptors. After synthesis in their high-mannose form, subunits mature within the ER into high-affinity pentameric receptors. Maturation involves oligomerization and folding events that allow the recognition between the β subunit and mAb290. After these processes, only pentameric receptors are allowed to traffic forward into the secretory pathway, through the Golgi apparatus where sugars are trimmed and processed into complex carbohydrates, to eventually reach the cell surface. According to our experiments, nicotine, which efficiently crosses the cell membrane, acts on the early maturation within the ER on an oligomeric species that possess an unknown stoichiometry αiβj. In regard to the location of the upregulation microdomain previously identified (Sallette et al., 2004) at the α/β interface (represented by a light gray square), we propose that nicotine binds to a nicotine-sensitive precursor and promotes a critical subunit-subunit interaction step that is limiting in the maturation of the α4β2 receptor.

### A Critical Role of Subunit-Subunit Interaction in the Upregulation Process

In the absence of nicotine, the weak maturation of α4β2 receptors is a priori related to their complex architecture. This implies sequential hetero-oligomerization steps, concomitant with folding of the extracellular and transmembrane domain and disulfide-bridge processing (Green and Millar, 1995). Yet, previous work pointed to a major role of subunit-subunit interaction in this inefficient maturation: (1) a 16 amino acid microdomain paving the α/β interface was found to govern the different expression and upregulation patterns of β2 and

β4 containing receptors (Sallette et al., 2004): α3/α4β2 receptors mature inefficiently and are strongly upregulated by nicotine, whereas α3/α4β4 receptors mature efficiently and are weakly upregulated, (2) an increased assembly of GFP-tagged α4 and β2 subunits inside the cells following nicotine upregulation was inferred from fluorescence energy transfer experiments (Nashmi et al., 2003), and (3) upregulation increased the coimmunoprecipitation between the Triton X-100 solubilized α3 and β2 subunits (Wang et al., 1998). Thus, the β2 subunit confers weak receptor maturation due to inefficient subunit interaction and/or assembly. This would result in a transient population of immature species called "nicotine-sensitive precursors," which are rapidly degradated in control conditions but rescued in the presence of nicotine. In regard to the fast kinetics of receptor maturation at 37°C, it is likely that within the 30 min of metabolic labeling these nicotine-sensitive precursors represent a small fraction of the total population, since the closely related mouse muscle-type nAChR has been shown to assemble in less than 20 min at 37°C (Green and Claudio, 1993).

Interestingly, while the concentration required to upregulate the receptors are 100- to 1000-fold higher than those required to occupy the agonist binding site at equilibrium, an excellent correlation between the $EC_{50}$ for upregulation and the $K_D$ for ligand binding was observed by many authors in several expression systems (Gopalakrishnan et al., 1997; Warpman et al., 1998; Whiteaker et al., 1998). These results suggest that the binding site for upregulation corresponds to the classical nicotine binding site that bridges the α/β subunit interface, but in an immature low-affinity conformation. Therefore, we propose that oligomeric immature entities displaying low but significant affinity for competitive ligands are the target for nicotine. Nicotine would bind to these precursors to stabilize a conformation possessing higher affinity for nicotine and facilitate progression to further steps of maturation toward high-affinity receptors. The particular location of the aforementioned microdomain, which bridges the nicotinic binding site and the subunit interface, suggests a molecular mechanism in which nicotine binds to the nicotine-sensitive precursor and stabilizes a conformation of the microdomain, strengthening the intersubunits interactions.

## Conclusion

We also found that the maturational enhancer mechanism investigated in transfected HEK293 cells also takes place in transfected SH-SY5Y neuroblastoma cells, in particular under low micromolar nicotine concentrations that are close to the nicotine concentrations found in the blood of smokers. These latter cells express several nAChRs and resemble human fetal sympathetic neurons grown in primary culture. This supports the conclusion that the maturational enhancer mechanism contributes to nicotine upregulation in animal models and possibly in the smoker.

As discussed in previous papers (Buisson and Bertrand, 2002; Dani and De Biasi, 2001), upregulation may have important consequences in the long-term effect of nicotine, possibly including nicotine sensitization, tolerance, and/or addiction, and possibly in schizophrenic disorders, since the brain of patients with schizophrenia present much less upregulation as compared to control smokers (Breese et al., 2000). The observation that upregulation produces an increase in nicotine-elicited release of dopamine within the mesolimbic pathway may be particularly important in addictive processes.

In addition, the observation that upregulation is a conserved feature among neuronal heteromeric nAChRs, particularly those containing the β2 subunit, is intriguing. We previously found that the compact microdomain from the β2 subunit that confers both low maturational efficacy and strong upregulation is highly conserved among species, including mouse, chick, rat, and human. This suggests that upregulation fulfills a specific physiological role. Our observation that choline strongly upregulates the α4β2 receptor, at concentrations compatible with those measured in the rat brain (between 10 and 20 μM under normal conditions, and to over 100 μM under pathological circumstances [Uteshev et al., 2003]) suggests that it may act as a positive maturational effector under physiological condition. In such a scheme, liberation of ACh from varicosities would lead to elevated levels of "ambient" ACh and/or choline, causing upregulation of nAChRs in the vicinity of the sites of neuromodulator liberation.

## Experimental Procedures

### Cell Culture, Transfection, and Upregulation

Human embryonic kidney HEK293 cells and SH-SY5Y neuroblastoma cells were cultured in Minimum Essential Medium containing 100 units/ml penicillin, 100 μg/ml streptomycin, 2 mM glutamine, and 10% fetal calf serum (Invitrogen) in a 5% $CO_2$ incubator at 37°C. Cells were grown in 90 mm dishes and transfected with the human α4 and β2 cDNA in the pRcCMV vector (Monteggia et al., 1995) using the calcium-phosphate method (Sallette et al., 2004) and were rinsed 24 hr after transfection. Upregulating ligands were added to the culture medium 24 hr after transfection, and experiments were performed 48 hr after transfection. In immunoprecipitation experiments, ligands at the same concentration were also present during the methionine deprivation, the metabolic labeling, and the chase periods. In binding and electrophysiological experiments, ligand-containing medium was replaced twice by ligand-free medium during 1 hr before the measurements to ensure their complete removal.

### Metabolic Labeling and Immunoprecipitation

Cells were treated for 20 min in methionine- and cystine-free DMEM (Invitrogen), labeled with 300 μCi/dish Redivue L-Pro-mix [$^{35}$S] (Amersham) and chased with methionine-containing medium. Cells were washed three times in PBS, harvested in 5 mM EDTA in PBS, centrifuged at 1500 rpm, solubilized overnight in 200 μl/dish ice-cold buffer A (150 mM NaCl, 50 mM Tris-Cl [pH = 8], 2 mM N-ethylmaleimide [Sigma], 5 mM EDTA, 1% lubrol, 1.83 mM mg/ml phosphatidylcholine [Sigma], and complete protease inhibitor cocktail [Roche]) (Green and Claudio, 1993) and centrifuged 10 min at 100,000 × g. Supernatant was precleared 30 min with 15 μl/dish protein G-coated dynabeads (Dynal) and incubated 24 hr at 4°C with mAb299 or mAb290 (Sigma) or anti-GFP (Invitrogen) at 1/200 dilution. 30 μl/dish dynabeads were added for 3 hr at 4°C, pelleted by centrifugation, washed four times in buffer A containing 1, 1, 0.5, or 0.15 mM NaCl (Cooper and Millar, 1997), detached for 10 min at 100°C using 20 μl/dish red loading buffer (Biolabs) containing 0.5 mM DTT and 5 μl SDS 20%. Endo-H and PNGase-F (Biolabs) digestions were performed for 1 hr at 37°C before the addition of 5 μl SDS 20%. The supernatant was loaded on a 7% Tris-Acetate NuPage gel (Invitrogen). The gel was fixed for 1 hr, incubated for 1

hr in En[$^3$H]ance (NEN), rinsed in water for 1 hr, and dried overnight at 37°C. Autoradiography was performed using Bio-Max MR films (Kodak) whose linearity was checked with Autoradiographic [$^{14}$C]micro-scales (Amersham). Quantification of the bands was performed by scanning densitometry. For the parallel mAb290 and anti-GFP immunoprecipitations, 30% and 70% of the material was respectively immunoprecipitated with anti-GFP and mAb290, and both fractions were pooled before solubilization in red loading buffer and loading on a 10% Bis-Tris NuPage gel.

### [$^3$H]-Epibatidine Binding

[$^3$H]-epibatidine was incubated with intact cells (respectively solubilized receptors) for 30 min at 37°C, filtered through GF/C filters preincubated in 1% milk powder solution (respectively, three superimposed GF/C filters preincubated in 1% polyethylene imine [Sigma]) (Sallette et al., 2004). The filters were incubated in BCS counting scintillant (Amersham) and counted in a LKB-Wallak counter.

### Immunofluorescence Labeling

HEK293 or SH-SY5Y cells transfected with cDNA of $\alpha$4, $\beta$2, and pECFP-Golgi Vector (Clontech) were cultured on glass coverslips pretreated with poly-L-lysine and fixed for 15 min with 4% formaldehyde at 37°C. All subsequent steps were performed at room temperature. Cells were permeabilized for 5 min with 0.2% Triton X-100. Nonspecific sites were blocked for 30 min with PBS containing 10% of goat serum. ER staining was performed according to the manufacturer's instructions (SelectFX Alexa fluor 488 Endoplasmic Reticulum Labeling kit, Molecular Probes). $\beta$2 subunit staining was performed with mAb 290, dilution 1/2500 for 90 min and incubation with a goat anti-rat IgG coupled to Alexa Fluor 568 (Molecular probes), dilution 1/1000, for 1 hr. After mounting coverslips with Vectashield mounting medium (Vector Laboratories), fluorescence was viewed under Zeiss confocal LSM 510 microscope.

### Analysis of Surface Receptors

Cells were incubated for 30 min at 4°C in PBS containing 0.5 mM sulfo-NHS-biotine (Uptima), rinsed in PBS and solubilized overnight in buffer A. After immunoprecipitation (as described above), the subunits were separated on a 7% Tris-acetate NuPage gel (Invitrogen) and transferred onto a nitrocellulose membrane (Amersham). After overnight saturation in PBS containing 0.5% milk powder, 1% BSA, and 0.05% Tween 20, blots were incubated in 1/2000 peroxydase-conjugated extravidine (Sigma) in the same buffer for 1 hr. After three washes, biotinylated cell surface receptors were revealed by the ECL+ (Amersham) procedure as described by the supplier.

### Sucrose Gradients

Metabolically labeled cells were solubilized overnight. After preclearing the cell lysate, the solution was loaded on an 11 ml 3%–30% (w/v) sucrose gradient in solubilization medium. Gradients were run in a SW 41 rotor (Beckman) 26 hr at 37 000 RPM at 4°C. 250 $\mu$l to 1 ml fractions were manually collected from the top of the gradient. Each fraction was immunoprecipitated as described above. For [$^3$H]-epibatidine analyzed gradients, the same procedure was performed on nonlabeled cells. Pentameric fraction was assessed by running the Torpedo receptor in parallel according to Nelson et al. (2003).

### Electrophysiology

Electrophysiological recordings were performed as previously described (Grutter et al., 2003). Briefly, macroscopic currents were recorded on HEK293 cells cotransfected with the $\alpha$4, $\beta$2, and green fluorescent protein cDNAs, using the whole-cell patch-clamp technique, at a holding potential of –60 mV. Only transfected cells (visualized with a fluorescent microscope for the presence of GFP) were tested.

### Supplemental Data

The Supplemental Data for this article can be found online at http://www.neuron.org/cgi/content/full/46/4/595/DC1/.

### Aknowledgments

We wish to thank Jean-Philippe Pin and Jean Cartaud for helpful remarks, Brian Molles for critical reading, and Uwe Maskos and Phillipe Faure for technical assistance. This work was supported by the Collège de France, the Commission of the European Communities (CEC), the Association pour la Recherche sur le Cancer, the Association Française contre les Myopathies, the Fondation pour la Recherche Médicale, and the Fondation Gilbert Lagrue.

Received: July 7, 2004
Revised: November 19, 2004
Accepted: March 24, 2005
Published: May 18, 2005

### References

Arroyo-Jimenez, M.M., Bourgeois, J.P., Marubio, L.M., Le Sourd, A.M., Ottersen, O.P., Rinvik, E., Fairen, A., and Changeux, J.P. (1999). Ultrastructural localization of the alpha4-subunit of the neuronal acetylcholine nicotinic receptor in the rat substantia nigra. J. Neurosci. *19*, 6475–6487.

Benwell, M.E., Balfour, D.J., and Anderson, J.M. (1988). Evidence that tobacco smoking increases the density of (-)-[$^3$H]nicotine binding sites in human brain. J. Neurochem. *50*, 1243–1247.

Breese, C.R., Lee, M.J., Adams, C.E., Sullivan, B., Logel, J., Gillen, K.M., Marks, M.J., Collins, A.C., and Leonard, S. (2000). Abnormal regulation of high affinity nicotinic receptors in subjects with schizophrenia. Neuropsychopharmacology *23*, 351–364.

Buisson, B., and Bertrand, D. (2001). Chronic exposure to nicotine upregulates the human $\alpha4\beta2$ nicotinic acetylcholine receptor function. J. Neurosci. *21*, 1819–1829.

Buisson, B., and Bertrand, D. (2002). Nicotine addiction: the possible role of functional upregulation. Trends Pharmacol. Sci. *23*, 130–136.

Christianson, J.C., and Green, W.N. (2004). Regulation of nicotinic receptor expression by the ubiquitin-proteasome system. EMBO J. *23*, 4156–4165.

Cooper, S.T., and Millar, N.S. (1997). Host cell-specific folding and assembly of the neuronal nicotinic acetylcholine receptor alpha7 subunit. J. Neurochem. *68*, 2140–2151.

Dani, J.A., and De Biasi, M. (2001). Cellular mechanisms of nicotine addiction. Pharmacol. Biochem. Behav. *70*, 439–446.

Ellgaard, L., and Helenius, A. (2003). Quality control in the endoplasmic reticulum. Nat. Rev. Mol. Cell Biol. *4*, 181–191.

Fenster, C.P., Whitworth, T.L., Sheffield, E.B., Quick, M.W., and Lester, R.A. (1999). Upregulation of surface $\alpha4\beta2$ nicotinic receptors is initiated by receptor desensitization after chronic exposure to nicotine. J. Neurosci. *19*, 4804–4814.

Gopalakrishnan, M., Monteggia, L.M., Anderson, D.J., Molinari, E.J., Piattoni-Kaplan, M., Donnelly-Roberts, D., Arneric, S.P., and Sullivan, J.P. (1996). Stable expression, pharmacologic properties and regulation of the human neuronal nicotinic acetylcholine $\alpha4\beta2$ receptor. J. Pharmacol. Exp. Ther. *276*, 289–297.

Gopalakrishnan, M., Molinari, E.J., and Sullivan, J.P. (1997). Regulation of human $\alpha4\beta2$ neuronal nicotinic acetylcholine receptors by cholinergic channel ligands and second messenger pathways. Mol. Pharmacol. *52*, 524–534.

Grailhe, R., de Carvalho, L.P., Paas, Y., Le Poupon, C., Soudant, M., Bregestovski, P., Changeux, J.P., and Corringer, P.J. (2004). Distinct subcellular targeting of fluorescent nicotinic alpha 3 beta 4 and serotoninergic 5–HT3A receptors in hippocampal neurons. Eur. J. Neurosci. *19*, 855–862.

Green, W.N., and Claudio, T. (1993). Acetylcholine receptor assem-

bly: subunit folding and oligomerization occur sequentially. Cell *74*, 57–69.

Green, W.N., and Millar, N.S. (1995). Ion-channel assembly. Trends Neurosci. *18*, 280–287.

Green, W.N., and Wanamaker, C.P. (1997). The role of the cystine loop in acetylcholine receptor assembly. J. Biol. Chem. *272*, 20945–20953.

Grutter, T., Prado de Carvalho, L., Le Novere, N., Corringer, P.J., Edelstein, S., and Changeux, J.P. (2003). An H-bond between two residues from different loops of the acetylcholine binding site contributes to the activation mechanism of nicotinic receptors. EMBO J. *22*, 1990–2003.

Harkness, P.C., and Millar, N.S. (2002). Changes in conformation and subcellular distribution of $\alpha4\beta2$ nicotinic acetylcholine receptors revealed by chronic nicotine treatment and expression of subunit chimeras. J. Neurosci. *22*, 10172–10181.

Kornfeld, R., and Kornfeld, S. (1985). Assembly of asparagine-linked oligosaccharides. Annu. Rev. Biochem. *54*, 631–664.

Lindstrom, J. (1996). Neuronal nicotinic acetylcholine receptors. In Ion channels, T. Narahashi, ed. (New York: Plenum Press), pp. 377–451.

Lukas, R.J., Norman, S.A., and Lucero, L. (1993). Characterization of nicotinic acetylcholine receptors expressed by cells of the SH-SY5Y human neuroblastoma clonal line. Mol. Cell. Neurosci. *4*, 1–12.

Marks, M.J., Burch, J.B., and Collins, A.C. (1983). Effects of chronic nicotine infusion on tolerance development and nicotinic receptors. J. Pharmacol. Exp. Ther. *226*, 817–825.

Merlie, J.P., and Lindstrom, J. (1983). Assembly in vivo of mouse muscle acetylcholine receptor: identification of an alpha subunit species that may be an assembly intermediate. Cell *34*, 747–757.

Monteggia, L.M., Gopalakrishnan, M., Touma, E., Idler, K.B., Nash, N., Arneric, S.P., Sullivan, J.P., and Giordano, T. (1995). Cloning and transient expression of genes encoding the human alpha 4 and beta 2 neuronal nicotinic acetylcholine receptor (nAChR) subunits. Gene *155*, 189–193.

Morello, J.P., Salahpour, A., Laperriere, A., Bernier, V., Arthus, M.F., Lonergan, M., Petaja-Repo, U., Angers, S., Morin, D., Bichet, D.G., and Bouvier, M. (2000). Pharmacological chaperones rescue cell-surface expression and function of misfolded V2 vasopressin receptor mutants. J. Clin. Invest. *105*, 887–895.

Nashmi, R., Dickinson, M.E., McKinney, S., Jareb, M., Labarca, C., Fraser, S.E., and Lester, H.A. (2003). Assembly of alpha4beta2 nicotinic acetylcholine receptors assessed with functional fluorescently labeled subunits: effects of localization, trafficking, and nicotine-induced upregulation in clonal mammalian cells and in cultured midbrain neurons. J. Neurosci. *23*, 11554–11567.

Nelson, M.E., Kuryatov, A., Choi, C.H., Zhou, Y., and Lindstrom, J. (2003). Alternate stoichiometries of $\alpha4\beta2$ nicotinic acetylcholine receptors. Mol. Pharmacol. *63*, 332–341.

Nguyen, H.N., Rasmussen, B.A., and Perry, D.C. (2003). Subtype-selective upregulation by chronic nicotine of high affinity nicotinic receptors in rat brain demonstrated by receptor autoradiography. J. Pharmacol. Exp. Ther. *307*, 1090–1097.

Nguyen, H.N., Rasmussen, B.A., and Perry, D.C. (2004). Binding and functional activity of nicotinic cholinergic receptors in selected rat brain regions are increased following long-term but not short-term nicotine treatment. J. Neurochem. *90*, 40–49.

Peng, X., Gerzanich, V., Anand, R., Whiting, P.J., and Lindstrom, J. (1994). Nicotine-induced increase in neuronal nicotinic receptors results from a decrease in the rate of receptor turnover. Mol. Pharmacol. *46*, 523–530.

Peng, X., Gerzanich, V., Anand, R., Wang, F., and Lindstrom, J. (1997). Chronic nicotine treatment upregulates $\alpha3$ and $\alpha7$ acetylcholine receptor subtypes expressed by the human neuroblastoma cell line SH-SY5Y. Mol. Pharmacol. *51*, 776–784.

Picciotto, M.R., Zoli, M., Rimondini, R., Lena, C., Marubio, L.M., Pich, E.M., Fuxe, K., and Changeux, J.P. (1998). Acetylcholine receptors containing the $\beta2$ subunit are involved in the reinforcing properties of nicotine. Nature *391*, 173–177.

Roth, B.L., Willins, D.L., and Kroeze, W.K. (1998). G protein-coupled receptor (GPCR) trafficking in the central nervous system: relevance for drugs of abuse. Drug Alcohol Depend. *51*, 73–85.

Rowell, P.P., and Wonnacott, S. (1990). Evidence for functional activity of upregulated nicotine binding sites in rat striatal synaptosomes. J. Neurochem. *55*, 2105–2110.

Sallette, J., Bohler, S., Benoit, P., Soudant, M., Pons, S., Le Novere, N., Changeux, J.P., and Corringer, P.J. (2004). An extracellular protein microdomain controls up-regulation of neuronal nicotinic acetylcholine receptors by nicotine. J. Biol. Chem. *279*, 18767–18775.

Schwartz, R.D., and Kellar, K.J. (1983). Nicotinic cholinergic receptor binding sites in the brain: regulation in vivo. Science *220*, 214–216.

Smith, M.M., Lindstrom, J., and Merlie, J.P. (1987). Formation of the alpha-bungarotoxin binding site and assembly of the nicotinic acetylcholine receptor subunits occur in the endoplasmic reticulum. J. Biol. Chem. *262*, 4367–4376.

Strecker, A., Franke, P., Weise, C., and Hucho, F. (1994). All potential glycosylation sites of the nicotinic acetylcholine receptor delta subunit from Torpedo californica are utilized. Eur. J. Biochem. *220*, 1005–1011.

Uteshev, V.V., Meyer, E.M., and Papke, R.L. (2003). Regulation of neuronal function by choline and 4OH-GTS-21 through alpha 7 nicotinic receptors. J. Neurophysiol. *89*, 1797–1806.

Wang, F., Nelson, M.E., Kuryatov, A., Olale, F., Cooper, J., Keyser, K., and Lindstrom, J. (1998). Chronic nicotine treatment up-regulates human $\alpha3\beta2$ but not $\alpha3\beta4$ acetylcholine receptors stably transfected in human embryonic kidney cells. J. Biol. Chem. *273*, 28721–28732.

Warpman, U., Friberg, L., Gillespie, A., Hellstrom-Lindahl, E., Zhang, X., and Nordberg, A. (1998). Regulation of nicotinic receptor subtypes following chronic nicotinic agonist exposure in M10 and SH-SY5Y neuroblastoma cells. J. Neurochem. *70*, 2028–2037.

Whiteaker, P., Sharples, C.G., and Wonnacott, S. (1998). Agonist-induced up-regulation of $\alpha4\beta2$ nicotinic acetylcholine receptors in M10 cells: pharmacological and spatial definition. Mol. Pharmacol. *53*, 950–962.

Whiting, P.J., and Lindstrom, J.M. (1988). Characterization of bovine and human neuronal nicotinic acetylcholine receptors using monoclonal antibodies. J. Neurosci. *8*, 3395–3404.